Supporting Information

Metal-ion-triggered symmetry breaking of completely achiral azobenzene amphiphile in water

Yun-Han Yang, Ran He, Yang Qin, and Ling Zhang*

PCFM Lab, IGCME, School of Chemistry, Sun Yat-Sen University, Guangzhou, 510275, China

E-mail: ceszl@mail.sysu.edu.cn

Table of Contents

1. Materials.

All commercial reagents were purchased from Energy Chemical, Acmec or Tansoole and were used as received. Unless otherwise noted, all starting materials and reagents were used without further purification. All aqueous solutions were prepared with deionized distilled water obtained from a Milli-Q water-purifying system (18 MΩ cm).

2. Instruments and Measurements.

The ^{1}H NMR spectra were recorded at 298 K on Bruker AVANCE III 400 MHz spectrometer using the residual solvent proton signal for calibration. Mass spectra (MS) were recorded on a thermo fisher scientific's Q exactive UHMR hybrid quadrupole-orbitrap mass spectrometer LC/MS (ESI). AFM imaging of samples prepared by dropping on a freshly cleaved mica were obtained on the Dimension FastScan Bio AFM. Circular dichroism (CD) spectra were recorded on a JASCO J1700 circular dichroism spectrometer in 1 mm path length quartz cuvette. AFM imaging of samples prepared by dropping on a freshly cleaved mica were obtained on the Dimension FastScan Bio AFM. The SEM images were recorded on a ZEISS Gemini 500 high-resolution thermal field emission scanning electron microscopy. The TEM instrument used was a JEOL JEM-2010 equipped with a Gatan 832 CCD camera. The samples of TEM and SEM were prepared at room temperature by placing a droplet on a formvar stabilized with carbon support film, and then the support film was blotted to remove the excess solution with filter paper. The FT-IR spectra were recorded using a PerkinElmer Frontier spectrophotometer, and the data was collected using an attenuated total reflection (ATR) unit. Weighing was performed on a Mettler EL204 analytical electronic balance.

3. Synthesis.

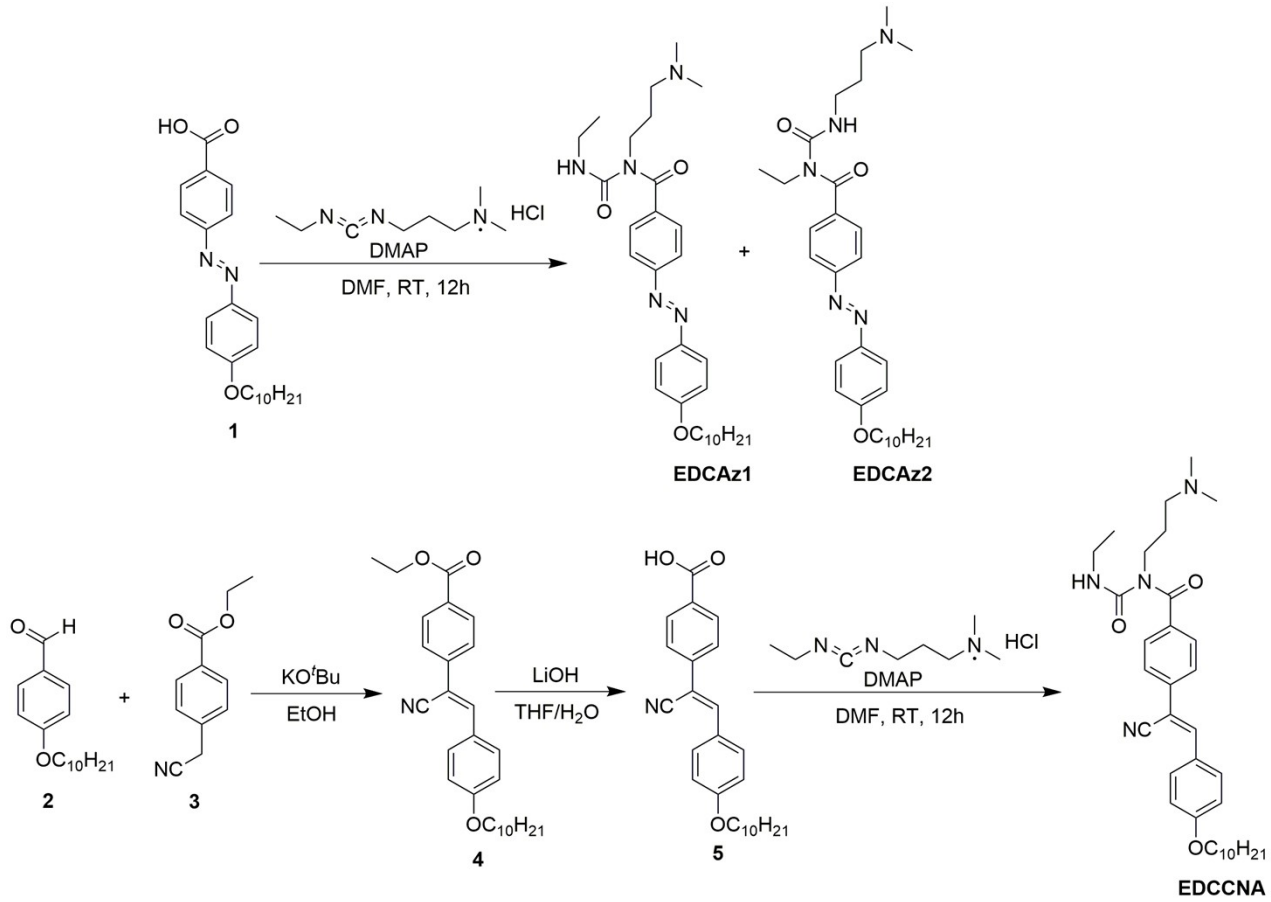

Scheme S1. Synthetic routes of EDCAz1, EDCAz2, and EDCCNA.

EDCAz1 was synthesized according to our previous report.[S1]

EDCAz2 was obtained as an isomer of **EDCAz1** by isolation (DCM/MeOH/TEA = 40:1:0.02, *v*/*v*/*v*, yield 20 %). **^{1}H NMR (600 MHz, $CDCl_3$):** δ 9.04 (t, *J* = 5.5, 1H), 7.92 (d, *J*=8.6, 4H), 7.56 (d, *J* = 8.3, 2H), 7.01 (d, *J* = 9.0, 2H), 4.05 (t, *J* = 6.6, 2H), 3.80 – 3.75 (m, 2H), 3.40 (q, *J* = 6.4, 2H), 2.40 (dd, *J* =8.2, 6.2, 2H), 2.26 (s, 6H), 1.82 (t, *J* = 7.4, 2H), 1.79 – 1.74 (m, 2H), 1.47 (t, *J* = 7.7, 2H), 1.34 – 1.25 (m, 12H), 1.13 (t, *J* = 7.0, 3H), 0.89 (d, *J* = 6.8, 3H). **^{13}C NMR (151 MHz, $CDCl_3$):** δ = 174.10, 162.43, 154.77, 153.67, 146.89, 137.88, 127.04, 125.25, 122.87, 114.95, 68.59, 57.54, 45.45, 44.84, 42.15, 39.26, 32.02, 29.69, 29.68, 29.50, 29.44, 29.30, 27.11, 26.13, 22.81, 15.14, 14.24. **HRMS (ESI):** *m/z* calculated for $[M+H]^+$ $C_{31}H_{48}N_5O_3^+$, 538.37517, found 538.37402.

The **compound 2** was synthesized according to literature procedure. [S2]

Synthesis of compound 5: The compound **2** (0.9 g, 3.44 mmol) and compound **3** (0.6 g, 3.44 mmol) were dissolved in anhydrous ethanol (50 mL), then anhydrous potassium tert-butoxide (0.3 g, 3.44 mmol) was added to the solution. After stirred overnight, white precipitate was obtained from the solution. After filtration, white powder (compound **4**) was obtained. This crude product was

dissolved in mixed solution (THF/H_2O = 3:1, v/v, 60.00 mL), LiOH (0.15 g, 6 mmol) was added, and then stirred at room temperature for 6 hours. A white solid suspension was obtained by adding hydrochloric acid to adjust pH to 2.0. The obtained white solid was filtered and dried under vacuum to give the crude product. Recrystallization in methanol afforded the white pure product compound **5**. **^{1}H NMR (400 MHz, DMSO-*d*6):** δ 13.14 (s, 1H), 8.11 (s, 1H), 8.03 (d, J = 8.6, 2H), 7.98 (d, J = 9.0, 2H), 7.86 (d, J = 8.5, 2H), 7.11 (d, J = 8.9, 2H), 4.06 (t, J = 6.5, 2H), 1.69 – 1.76 (m, 2H), 1.38 – 1.44 (m, 2H), 1.36 – 1.18 (m, 14H), 0.87 – 0.83 (m, 3H). **^{13}C NMR (100 MHz, DMSO-*d*6):** δ = 166.78, 161.07, 144.36, 138.30, 131.59, 130.61, 130.10, 125.86, 125.57, 118.19, 115.04, 105.84, 67.85, 31.33, 29.03, 28.98, 28.76, 28.73, 28.55, 25.47, 22.13, 14.00. **HRMS (ESI):** *m/z* calculated for $[M-H]^-$ $C_{26}H_{30}NO_3^-$, 404.22312, found 404.22388.

Synthesis of EDCCNA: The compound **5** (0.389 g, 1 mmol), EDCI (0.38g, 2 mmol) and DMAP (0.061g, 0.5 mmol) were dissolved in DMF (20 mL) at room temperature. The reaction was allowed to continue stirring for 12 hours. The crude product was diluted with water (30 mL) and then extracted with EDCI (3 × 15 mL) and washed with saturated aqueous NaCl (3 × 50 mL). The organic phase was dried over $MgSO_4$ and concentrated in vacuo by rotary evaporation. Purification via column chromatography (DCM: MeOH: TEA=50:1:0.25) to obtain **EDCCNA** as a white solid (0.35 g, 50%). **^{1}H NMR (400 MHz, DMSO-*d*6):** δ 8.72 (t, J = 5.4, 1H), 8.04 (s, 1H), 7.96 (d, J = 8.9, 2H), 7.77 (d, J = 8.5, 2H), 7.57 (d, J = 8.5, 2H), 7.10 (d, J = 8.9, 2H), 4.05 (t, J = 6.5, 2H), 3.67 (t, J = 6.8, 2H), 2.89 – 3.03 (m, 2H), 2.28 (t, J = 6.7, 2H), 2.15 (s, 6H), 1.72 (q, J = 6.8, 4H), 1.44 – 1.36 (m, 2H), 1.22 – 1.29 (m, 14H), 0.92 (t, J = 7.2, 3H), 0.84 (t, J = 6.8, 3H). **^{13}C NMR (100 MHz, DMSO-*d*6):** δ = 170.21, 160.94, 156.02, 143.62, 136.68, 136.10, 131.46, 127.92, 125.94, 125.11, 118.25, 115.01, 105.99, 67.84, 55.54, 44.95, 44.55, 43.86, 34.92, 31.34, 29.04, 28.99, 28.77, 28.74, 28.56, 25.48, 25.31, 22.14, 14.19, 14.00. **HRMS (ESI):** *m/z* calculated for $[M+ H]^+$ $C_{34}H_{49}N_4O_3^+$, 561.37992, found 561.37854.

4. Self-assembly Experiments.

The sample (EDCAz1, EDCAz2, or EDCCNA) (0.016mmol) was weighed into a pointed glass test tube and HCl aqueous solution (1 mL, 16 mmol/L) was added. The resulting mixture was further sonicated for 30 min until a clear orange solution was obtained. Subsequently, the metal ions (0.08 mmol) were added, and the mixture was further sonicated for 30 min. Finally, the solution was stood in the dark at room temperature.

5. Evaluation of LD Contribution.

In order to evaluate the contribution of LD to ECD, LD, and ECD spectra have been simultaneously measured as previous reports [S5-S8]. The apparent ECD (CD_{app}) could be expressed by the following Equation S1:

$$CD_{app} = CD_{true} + LD\cos 2\beta_0 \sin k + 1/6[CB\ LD\ LB - \mathrm{CD}\ LB_2 + (1/2\ln 10)_2(CD_3 + CD\ LD_2)] \quad \textbf{S1}$$

Where CD_{true} denotes the true CD signal, κ is the static birefringence of the modulator orientated at the angle β_0 to the axis system of the induced birefringence. CB and LB denote the circular and linear birefringence, respectively. The influence of the term in square brackets on the apparent CD signal can be assumed to be small compared to the second term, since it contains higher products of the small terms CB and CD. [S5, S6] For a CD spectrometer equipped with a photoelastic modulator (PEM), the factor $\cos 2\beta 0 \sin\kappa$ is approximately 0.02. [S5,S8] Therefore, the Equation (S1) can be approximatively written as Equation (S2):

$$CD_{\mathrm{app}} = CD_{\mathrm{true}} + LD \times 0.02 \quad \textbf{S2}$$

The true CD signals can be calculated by the following semi-empirical equation, Equation S3:

$$CD_{\mathrm{true}} = CD_{\mathrm{app}} - LD \times 0.02 \quad \textbf{S3}$$

6. Job′s plot

The stoichiometry of the complex between EDCAz1 and Zn^{2+} was determined by Job′s plot method.[S3] In this method, we kept the total molar concentrations of EDCAz1 and Zn^{2+} constant and continuously varied the molar fraction of EDCAz1 and Zn^{2+}. The absorbance of each mole fraction was measured at 399 nm, and the Job′s curve was plotted.

7. Computational Details.

The structures of EDCAz1, EDCAz2, EDCCNA, EDCAz1/Zn^{2+}, EDCAz1-dimer, EDCAz1/Zn^{2+} – dimer with *P*-helix stacking, and EDCAz1/Zn^{2+} – dimer with *M*-helix stacking were optimized at the M06-2X/LANL2DZ ~ 6–31G(d) computational level with the IEFPCM solvation method in water. We have verified the stability of the optimized structures by using vibrational analysis (no imaginary vibrations). ECD calculations were performed at the M06-2X/LANL2DZ ~ 6–31G (d) level of theory with TD-DFT computing transitions to the lowest 100 electronically excited singlet states. VCD calculations were performed at the M06-2X/LANL2DZ ~ 6–31G (d) level of theory. In the calculation process, the 6-31G (d) basis set was used for C, H, O, N, and Cl, whereas LANL2DZ was used for Zn. All calculations were carried out using Gaussian 09 software. [S4]

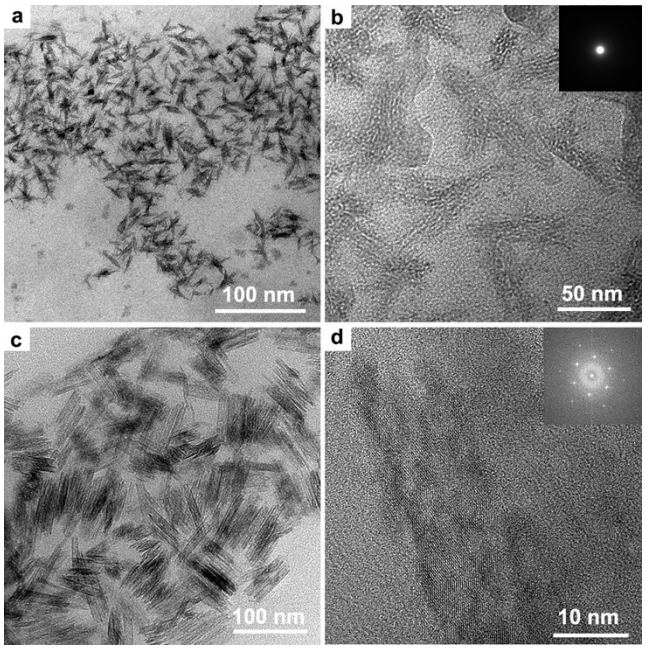

Fig. S1 TEM images of cationic EDCAz1/Fe^{3+} system; shuttle-like nanosheets (a, b) and nanotubes (c, d); inset in (b, d) is the fast Fourier transformation (FFT) pattern.

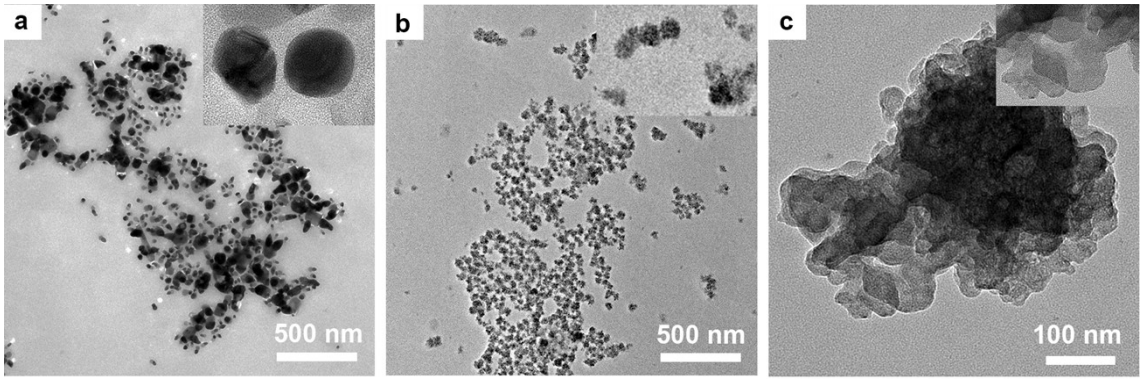

Fig. S2 TEM images of cationic EDCAz1/Al^{3+} (a), cationic EDCAz1/Cu^{2+} (b), and cationic EDCAz1/Ca^{2+} (c).

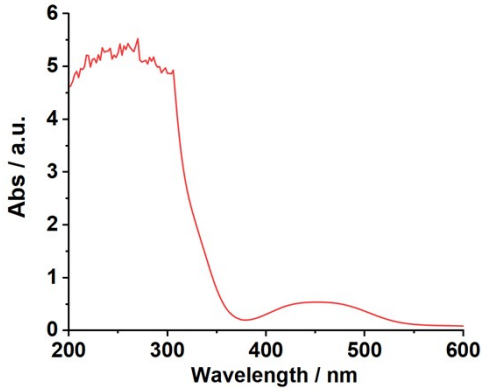

Fig. S3 Absorption spectra of $PdCl_2$ in dilute hydrochloric acid aqueous solution

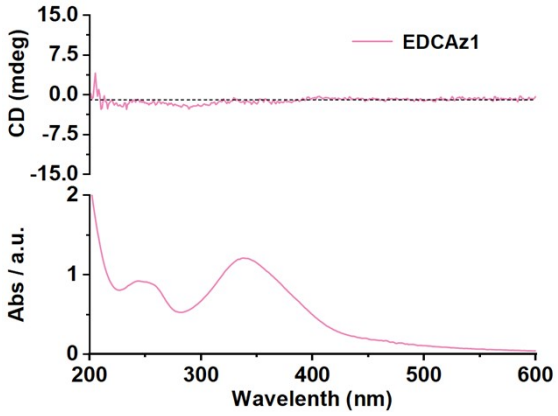

Fig. S4 CD spectra of cationic EDCAz1.

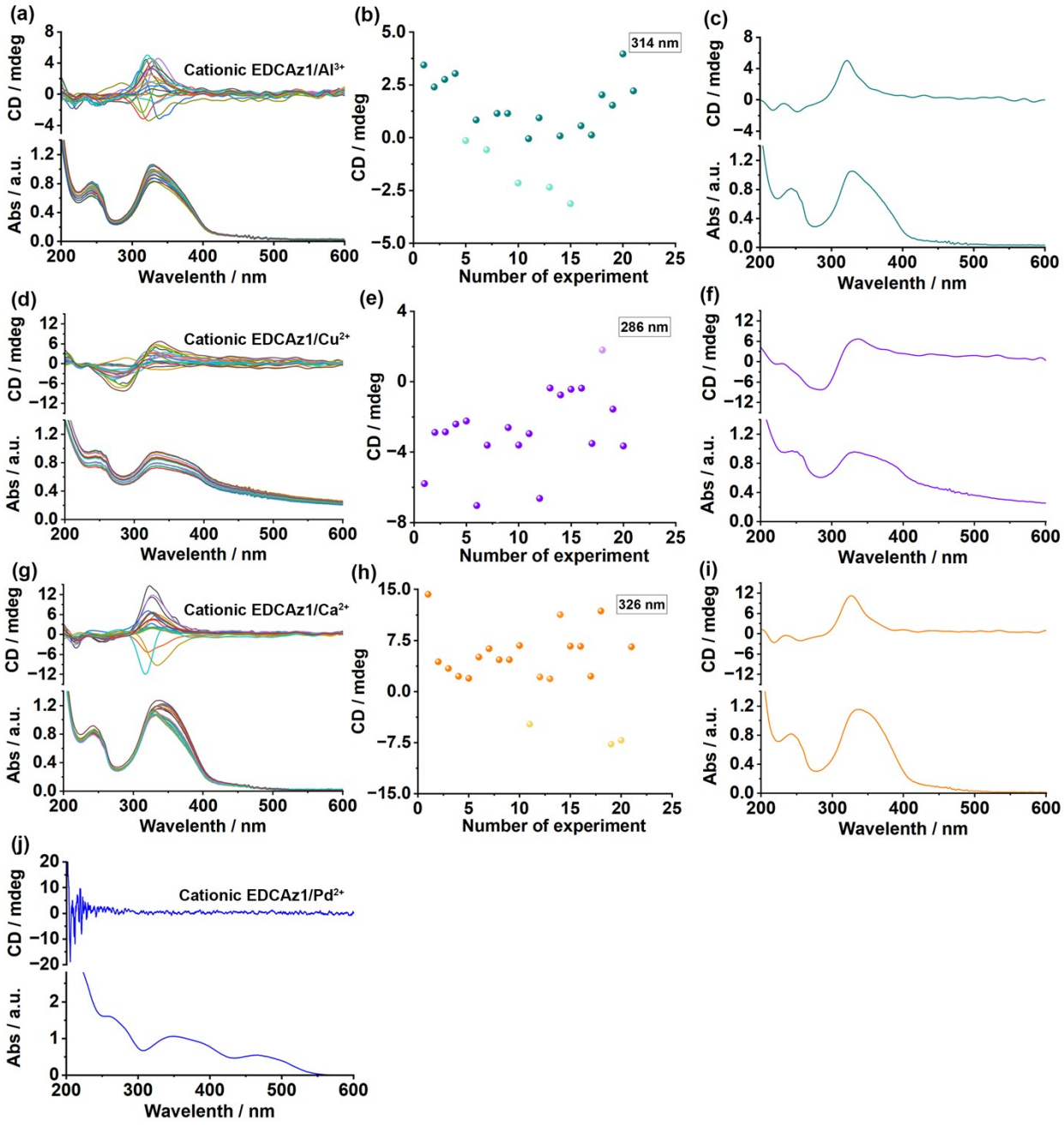

Fig. S5 CD spectra of cationic EDCAz1/Al^{3+} (a, b, and c), cationic EDCAz1/Cu^{2+} (d, e, and f), cationic EDCAz1/Ca^{2+} (g, h, and i), and cationic EDCAz1/Pd^{2+} (j).

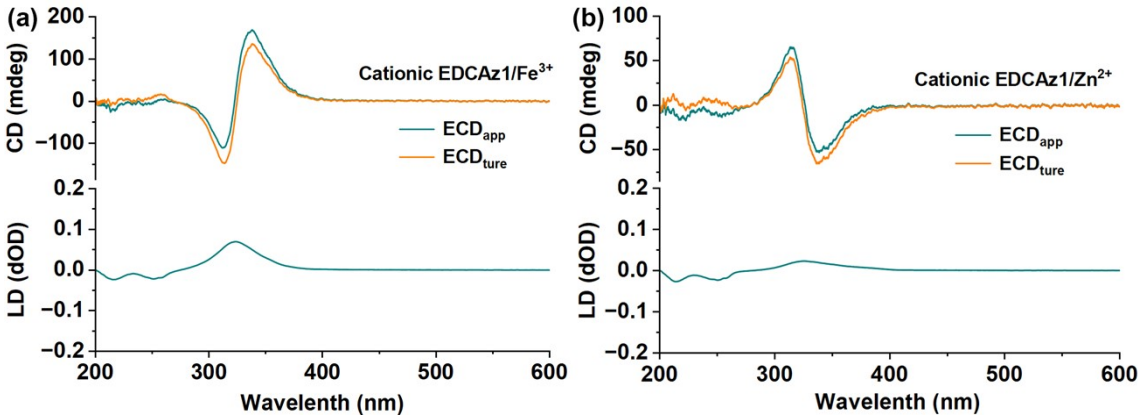

Fig. S6 The contribution of LD to ECD is assessed as represented by cationic EDCAz1/Fe^{3+} and cationic EDCAz1/Zn^{2+} systems.

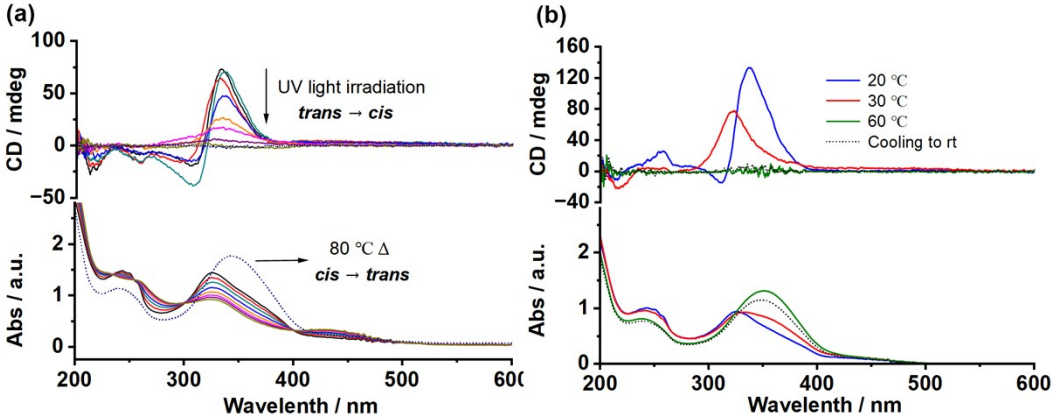

Fig. S7 ECD changes of representive cationic EDCAz1/Fe^{3+} by *trans-cis-trans* isomerization (a) and heating-cooling stimuli (b).

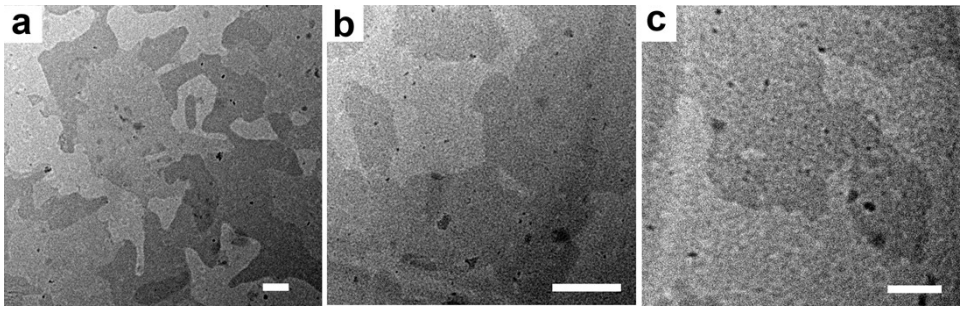

Fig. S8 TEM images of cationic EDCAz2 (a), cationic EDCAz2/Zn^{2+} (b), cationic EDCAz2/Fe^{2+} (c); Scale bars, 200 nm.

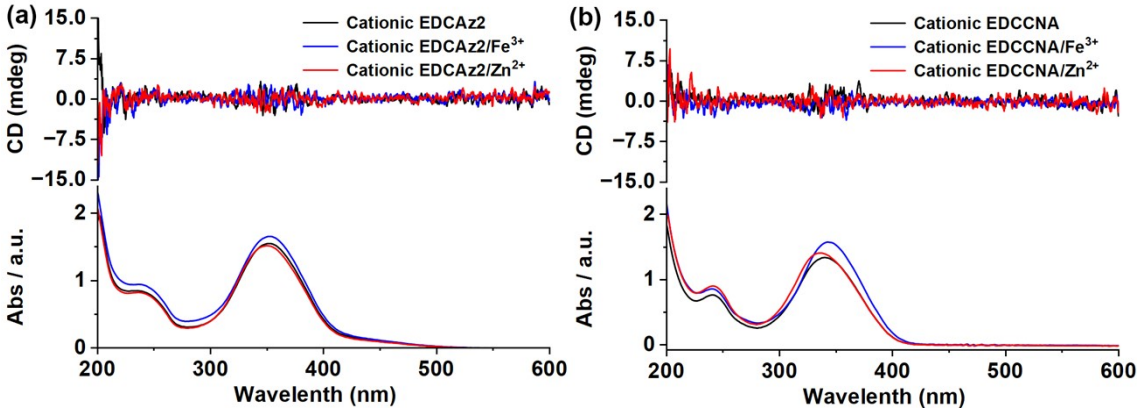

Fig. S9 CD spectra of cationic EDCAz2, cationic EDCAz2/Fe^{2+}, and cationic EDCAz2/Zn^{2+} (a); CD spectra of cationic EDCCNA, cationic EDCCNA/Fe^{2+}, and cationic EDCCNA/Zn^{2+} (a).

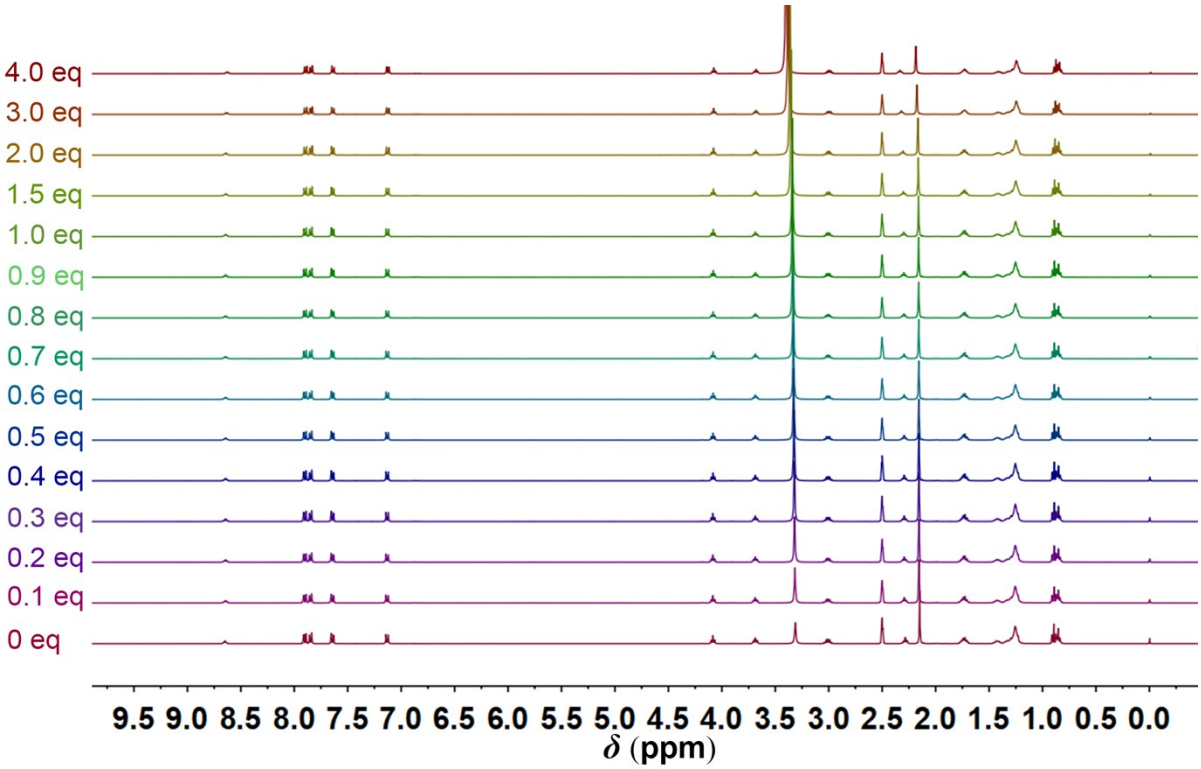

Fig. S10 ^{1}H NMR spectra of EDCAz1 in DMSO-*d*6 with the addition of different equiv. of Zn^{2+}. (EDCAz1 was dissolved in DMSO-*d*6 followed by the sequential addition of $Zn(NO_3)_2 \cdot 6H_2O$ in DMSO-d6.)

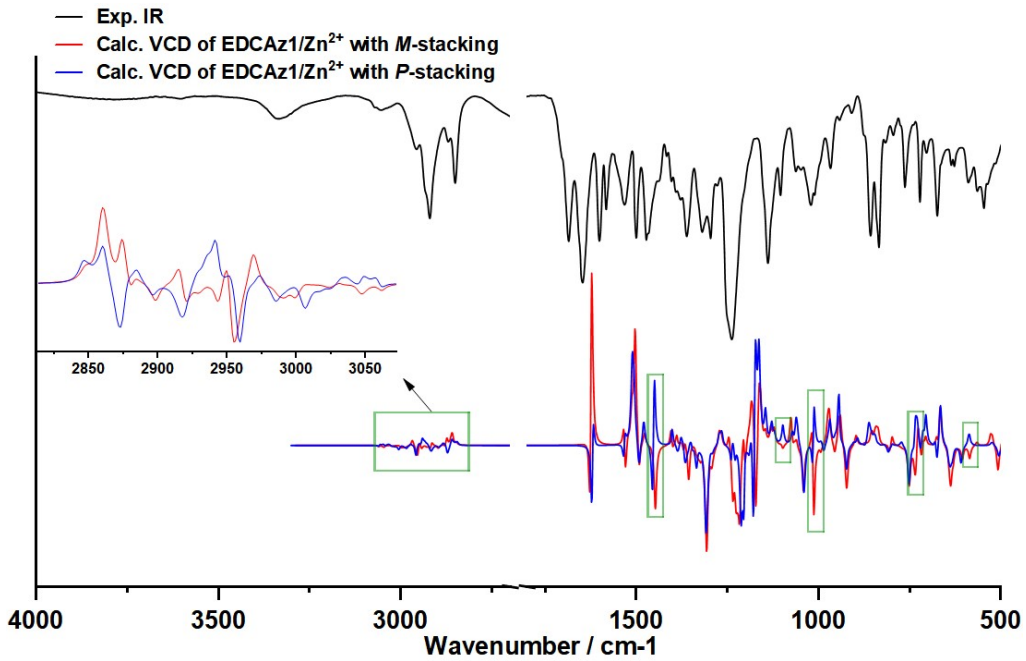

Fig. S11 Comparison of experimental infrared absorption spectroscopy with computed vibrational circular dichroism.

8. ^{1}H NMR and ^{13}C NMR Spectra.

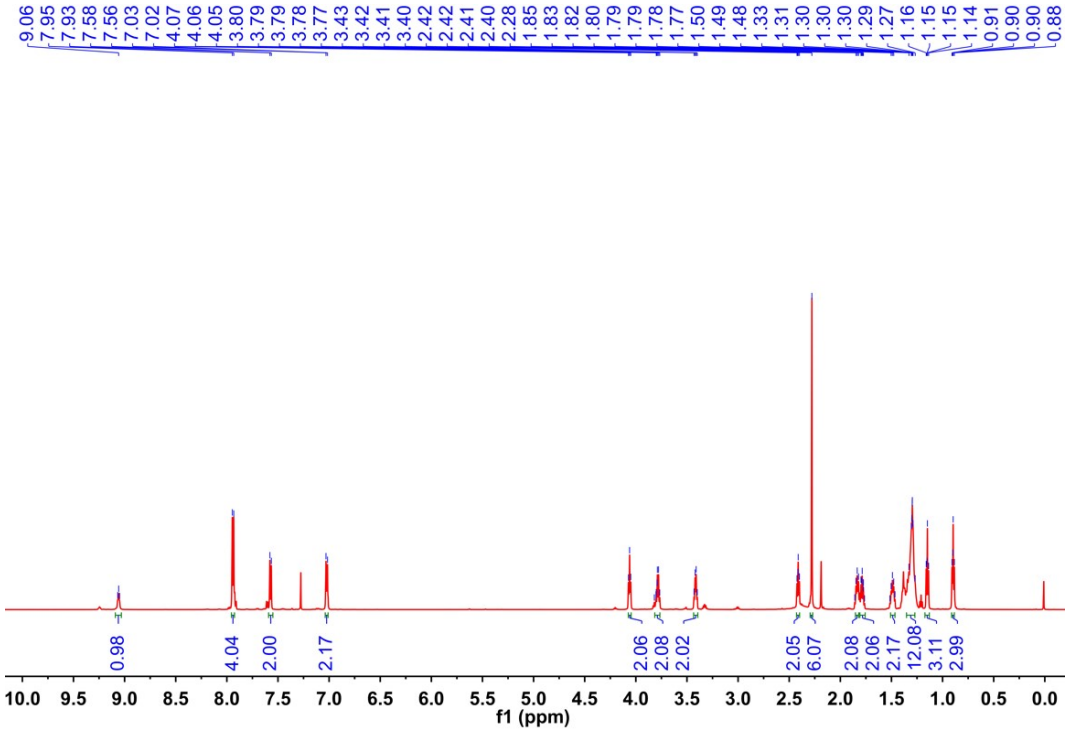

Fig. S12 ^{1}H NMR spectrum (400 MHz) of EDCAz2 in $CDCl_3$ at 25 °C.

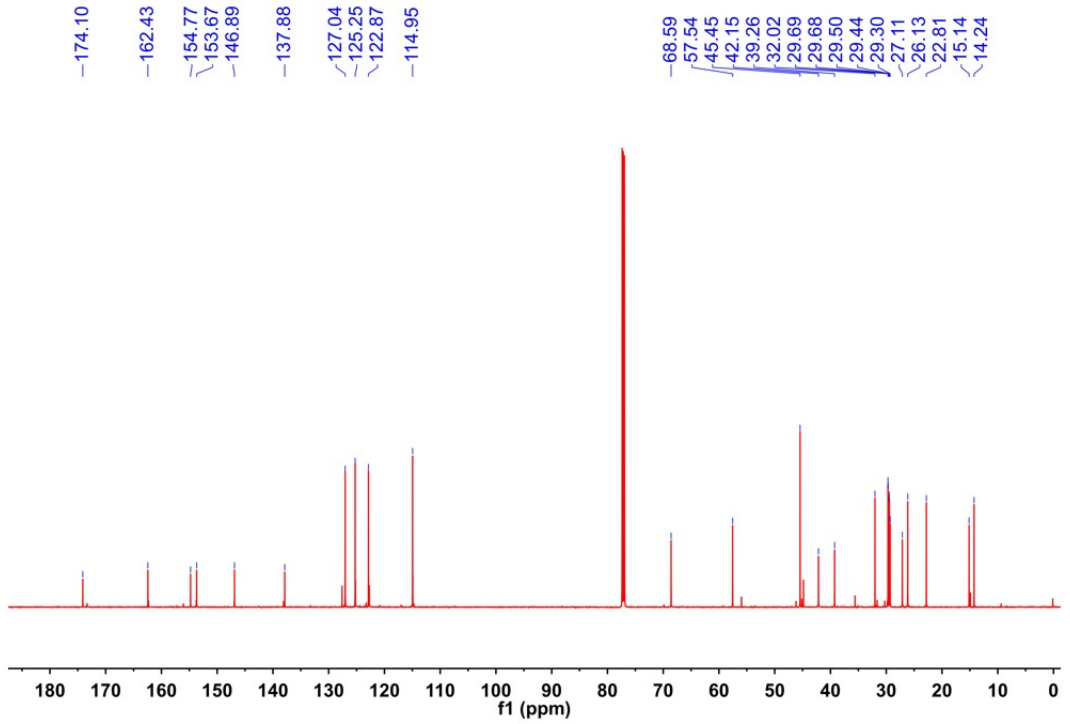

Fig. S13 ^{13}C NMR spectrum (100 MHz) of EDCAz2 in $CDCl_3$ at 25 °C.

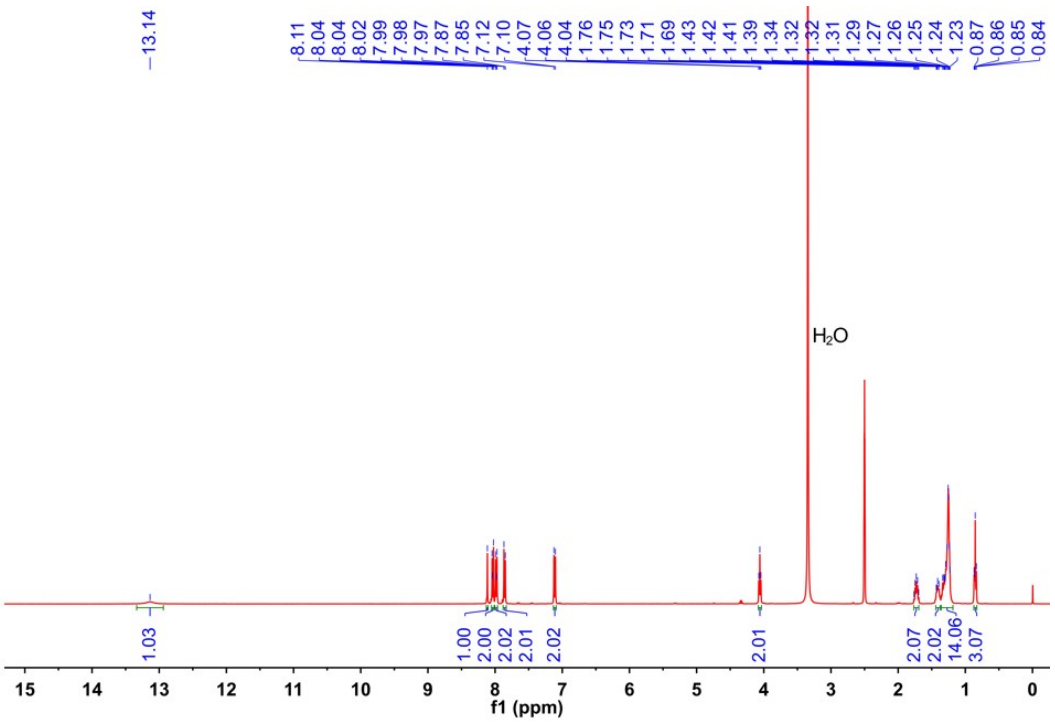

171

172 **Fig. S14** [1]H NMR spectrum (400 MHz) of compound **5** in DMSO-*d6* at 25 °C.

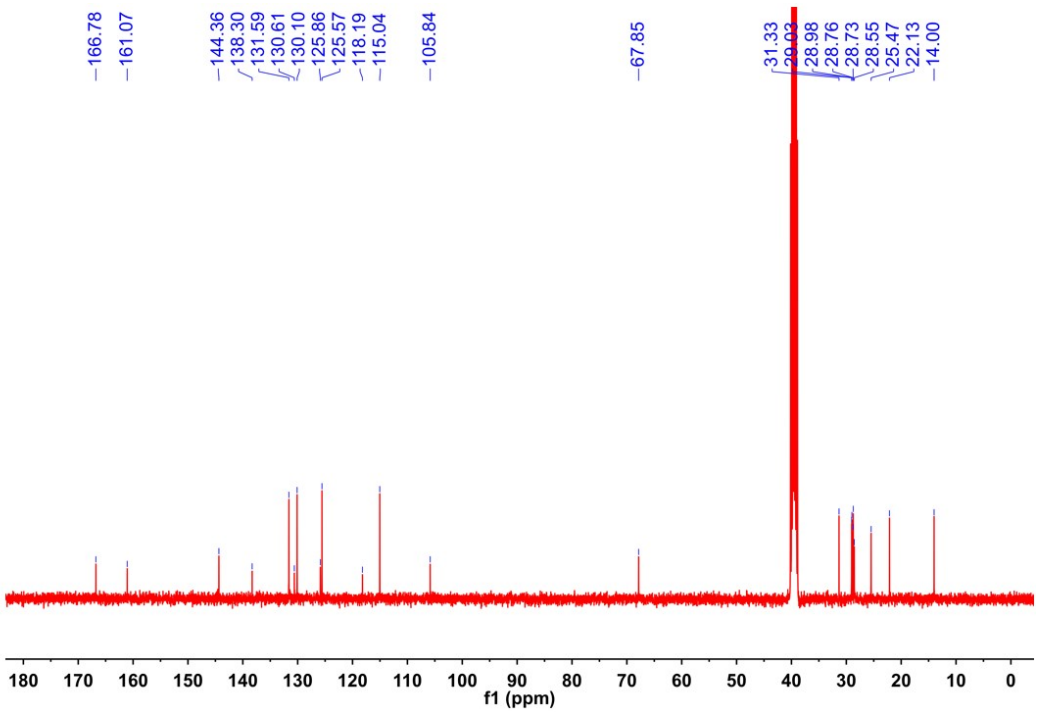

173

174 **Fig. S15** [13]C NMR spectrum (100 MHz) of compound **5** in DMSO-*d6* at 25 °C.

175

176

177

178

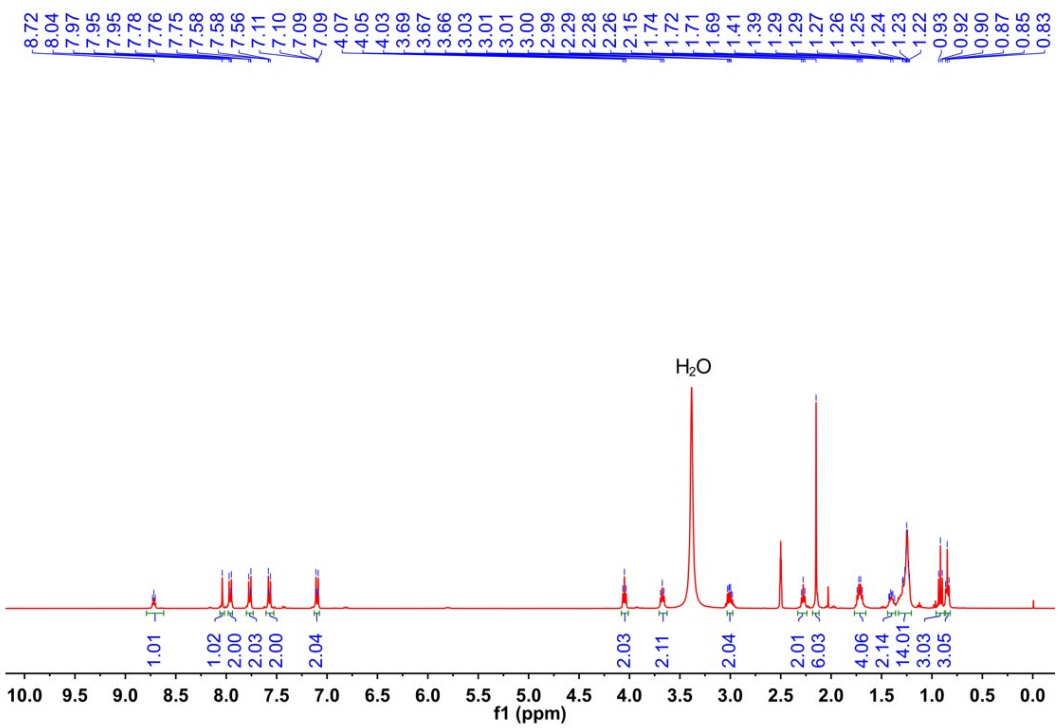

Fig. S16 ^{1}H NMR spectrum (400 MHz) of EDCCNA in DMSO-*d6* at 25 °C.

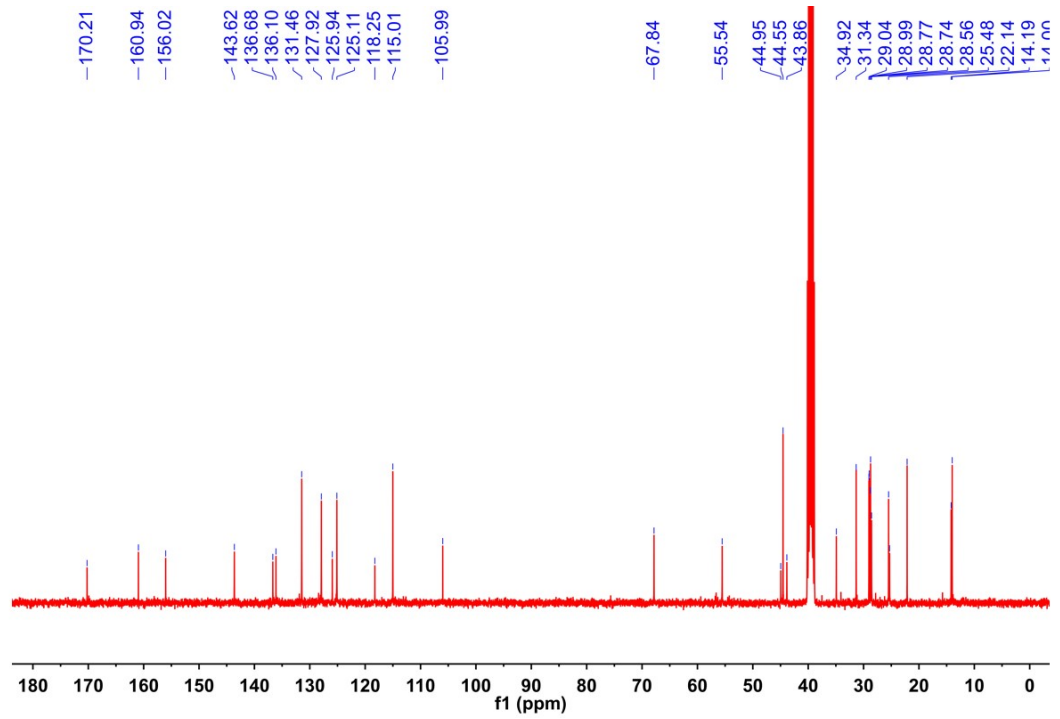

Fig. S17 ^{13}C NMR spectrum (100 MHz) of EDCCNA in DMSO-*d6* at 25 °C.

References.

[S1] L. Zhang, L. Zhou, N. Xu, and Z. Ouyang, Angew. Chem. Int. Ed. 2017, 56, 8191 - 8195.

[S2] J. Abdulkareem Abbas and Y. Yıldırır, J. Mol. Struct. 2023, 1281, 135050.

[S3] L. -J. Yang, Q. Chang, S. -Y. Zhou, Y. -H. Yang, F. -T. Xia, W. Chen, M. Li and X. -D. Yang. Dyes Pigments. 2018, 150, 193 - 201.

[S4] M. J. Frisch, G. W. Trucks, H. B. Schlegel, G. E. Scuseria, M. A. Robb, J. R. Cheeseman, G. Scalmani, V. Barone, B. Mennucci, G. A. Petersson, H. Nakatsuji, M. Caricato, X. Li, H. P. Hratchian, A. F. Izmaylov, J. Bloino, G. Zheng, J. L. Sonnenberg, M. Hada, M. Ehara, K. Toyota, R. Fukuda, J. Hasegawa, M. Ishida, T. Nakajima, Y. Honda, O. Kitao, H. Nakai, T. Vreven, J. A. Montgomery, Jr., J. E. Peralta, F. Ogliaro, M. Bearpark, J. J. Heyd, E. Brothers, K. N. Kudin, V. N. Staroverov, R. Kobayashi, J. Normand, K. Raghavachari, A. Rendell, J. C. Burant, S. S. Iyengar, J. Tomasi, M. Cossi, N. Rega, J. M. Millam, M. Klene, J. E. Knox, J. B. Cross, V. Bakken, C. Adamo, J. Jaramillo, R. Gomperts, R. E. Stratmann, O. Yazyev, A. J. Austin, R. Cammi, C. Pomelli, J. W. Ochterski, R. L. Martin, K. Morokuma, V. G. Zakrzewski, G. A. Voth, P. Salvador, J. J. Dannenberg, S. Dapprich, A. D. Daniels, Ö. Farkas, J. B. Foresman, J. V. Ortiz, J. Cioslowski, and D. J. Fox, Gaussian 09, Revision D.01, Gaussian, Inc., Wallingford CT, 2009.

[S5] H. Gillgren, A. Stenstam, M. Ardhammar, B. Nordón, E. Sparr, S. Ulvenlund, Langmuir 2002, 18, 462 - 469.

[S6] A. Ohira, K. Okoshi, M. Fujiki, M. Kunitake, M. Naito, Adv. Mater. 2004, 16, 1645 - 1650.

[S7] G. Gottarelli, S. Lena, S. Masiero, S. Pieraccini, G. P. Spada, Chirality 2008, 20, 471 - 485.

[S8] Å. Davidsson, B. Nordén, S. Seth, Chem. Phys. Lett. 1980, 70, 313 - 316.